Toward Sensing, Communications and Control Architectures for Frequency Regulation in Systems with Highly Variable Resources

Marija Ilić and Qixing Liu

Dedicated to Joe Chow, a true pioneer in rethinking sensing, communications and control of complex electric energy systems.

Abstract The basic objective of this chapter is to rethink frequency regulation in electric power systems as a problem of cyber system design for a particular class of complex dynamical systems. It is suggested that the measurements, communications and control architectures must be designed with a clear understanding of the temporal and spatial characteristics of the power grid as well as of its generation and load dynamics. The problem of Automatic Generation Control (AGC) and frequency regulation design lends itself well to supporting this somewhat general observation because its current implementation draws on unique structures and assumptions common to model aggregation in typical large scale dynamic network systems. We describe how these assumptions are changing as a result of both organizational and technological industry changes. We propose the interaction variable-based modeling framework necessary for deriving models which relax conventional assumptions when that is needed. Using this framework we show that the measurements, communications and control architectures key to ensuring acceptable frequency response depend on the types of disturbances, the electrical characteristics of the interconnected system and the desired technical and economic performance. The simulations illustrate several qualitatively different electric energy systems. This approach is by and large motivated by today's AGC and its measurement, communications and control architectures. It is with this in mind that we refer to our interaction variable-based frequency regulation framework as "enhanced AGC" (E-AGC). The enhancements come from accounting for temporal and spatial characteristics of the system which require a more advanced frequency regulation design than the one presently in place. Our proposed interaction variable-based aggregation modeling could form the basis for a coordination of interactions between the smart balancing authorities (SBAs) responsible for frequency regulation in the changing industry. Given the rapid deployment of synchrophasors, the proposed E-AGC can be easily implemented.

Marija Ilić
Carnegie Mellon University, 5000 Forbes Ave. Pittsburgh PA, 15213, e-mail: milic@ece.cmu.edu

Qixing Liu
Carnegie Mellon University, 5000 Forbes Ave. Pittsburgh PA, 15213, e-mail: lqx@cmu.edu

1 Introduction

A high quality of electricity service assumes near-ideal nominal frequency, which is the result of almost instantaneous power supply and demand balancing. In actual systems, deviations from this perfect balance always exist and are mainly caused by hard-to-predict demand and by the lack of direct power control exchange between neighboring utilities. Therefore, the resulting frequency must be regulated back to nominal by means of output feedback control responding to the frequency errors caused by the power imbalances. Much is known about AGC, and this control scheme is considered one of the most ingenious elegant feedback schemes in large-scale man-made network systems. Its effectiveness comes from viewing the problem as quasi-stationary and accounting for the fact that, at equilibrium, the system operates at a single frequency. This, together with the assumption that utilities are weakly connected, forms the basis for using Area Control Error (ACE) as the single output to which several fast-responding power plants respond in each utility (control area) and drive the error to zero within 10 minutes or so. It can be shown that, at theoretical equilibrium, the entire interconnected system will balance and frequency should return to nominal, provided that each control area responds to its own ACE without communicating with other control areas.

However, the question of ”correct” AGC standards and a utility’s ability to meet these standards has been a long-standing subject of many industry committees led by the North American Electric Reliability Organization (NERO). Many of the industry’s great thinkers, starting with the late Nathan Cohn, the father of AGC, have brought the scheme to near perfection over the years. Understanding the fundamentals of AGC, including the elusive notions of Inadvertent Energy Exchange (IEE) and Time Error Correction (TEC), requires an in-depth treatment which is outside the objectives of this chapter; the interested reader should explore the extensive literature on this subject. Ensuring that the standards are met has been difficult up until very recently because of the lack of synchronized measurements. As a result, there have been growing concerns about the worsening of frequency quality. These concerns have become magnified with the prospects of deploying highly variable energy resources, such as wind and solar power farms. This overall situation requires a rethinking of today’s AGC industry practice from the viewpoint of the key assumptions underlying its design. In particular, given the recent deployments of synchrophasor technologies capable of providing fast and synchronized measurements across wide areas, the question of an enhanced AGC (E-AGC) design and its purpose presents itself quite forcefully.

In this chapter we pose the problem of E-AGC as a control design problem based on a carefully designed dynamic model directly relevant for frequency regulation in complex power systems. We derive a model which can capture the effects of disturbances likely to be seen in future electric power systems with many intermittent resources. We observe that today’s AGC is used for the fine tuning of frequency deviations caused by small hard-to-predict power imbalances around the generation dispatched to supply forecast demand. As such, it is viewed as regulating steady-state frequency offsets over the time interval of 10-15 minutes; primary governor control at the same time compensates for local fluctuations very quickly, without considering dynamic interactions with the rest of the system. Simplicity is achieved by having fast local primary control which is tuned without modeling fast dynamic interactions with the rest of the system. AGC, on the other hand, compensates for steady-state net power imbalances in each utility, assuming that the electrical distances between the generators in the control area are negligible; the effects of other control areas are compensated for by responding to the Area Control Error, which is a measure of the power imbalance created by the internal demand deviations from the forecast and the deviations in net power exchange from the scheduled exchanges at the time of dispatch in each control area.

In emerging electric energy systems the implied spatial simplifications when designing fast-stabilizing primary control, as well as the implied temporal simplifications assuming near steady-state conditions when performing AGC and accounting for the effects of net imbalances within a large multi-control area interconnected power system, will become hard to justify. Depending on the electrical properties of the system, the nature of the disturbances causing the frequency changes, and the dynamics of the power plants and loads, it is plausible that frequency response may become very different than the historic response has been. Models for analyzing and predicting the likely frequency response and, consequently, designing controls for stabilizing and regulating frequency has become a very difficult problem. A power system driven by continuously varying persistent disturbances does not lend itself well to separating stabilization and regulation objectives.

In order to begin to answer these difficult questions, we pose in Section 2 the problem of frequency regulation by first reviewing a general dynamic model of an interconnected power system with typical system response to these new disturbances. To start with, this general model is very complex and without obvious structure. In Section 3 we propose a systematic model reduction which lends itself well to the enhanced frequency regulation design. Of particular interest is the derivation of models capable of capturing dynamic interactions between (groups of) system users given the ultimate objective of designing the minimum coordination architecture across these groups of system users necessary to control power imbalance interactions causing potentially unacceptable frequency response. Notably, the concepts introduced early on by Joe Chow and his collaborators for model reduction in electric power systems are shown to be key to arriving at the models for enhanced frequency regulation of interest here. Model simplification using standard singular perturbation is used to introduce acceptable temporal simplifications of the generator models used. Similarly, the lesser-known non-standard singular perturbation method is used to prove the existence of the interaction variable which can capture the dynamics of power imbalances across large power grid interconnections. The question of aggregation within an interconnected system and the implications of the grouping selected at the achievable frequency quality and the complexity of the required sensing, communications and control architectures is discussed in considerable detail. We recognize that aggregation principles could be based on : (1) the pre-defined organizational boundaries of the consumers and producers responsible for balancing supply and demand; the most typical representatives are utilities and/or control areas; (2) the bottom-up created portfolio of users and producers; representatives of such aggregated system users can likely be be entities comprising users with their own distributed energy resources; and, (3) best technical decomposition of a given dynamical system from the point of view of having coherent dynamic response and being controllable and observed without relying on help from the others. In Section 4 the model relevant for frequency regulation of each SBA is simulated to show the qualitatively different interaction variables resulting from the different relative electrical distances internal and external to the SBAs. In Section 5 we illustrate the use of coherency-based method introduced by Joe Chow for the four qualitatively different physical systems for seemingly identical design. We show the system aggregation which results from this approach. In Section 6 we compare the aggregation obtained using our proposed interaction variable-based modeling of SBAs with coherency-based aggregation. Interestingly, when inquiring whether interconnection-level coordination may be needed, the two methods arrive at the same conclusion via different paths. For SBAs with strong internal interactions the coherency-based method leads to the conclusion that a meaningful aggregation would be to have one single system. The interaction variable-based approach concludes that, because the interactions are strong, it is essential to coordinate them. Notably, the model proposed here does not neglect the effects of electrical distances; this is in sharp contrast with today's AGC. We show how the interaction variables are affected by the relative strength of electrical interconnections, both internal to the SBA and also in-between the SBAs.

We next show how these qualitatively different cases lend themselves to different measurement, communications and control architectures. In Section 7 a required sensing, communications and control architecture based on the interaction variable-based model is drawn up, and the results of using such a control architecture are illustrated for the four cases of a small system studied. In Section 8 a required sensing, communications and control architecture based on coherency-based aggregation is sketched out. The complexity of the two, and a comparison of the two, are summarized. In Section 9 we discuss the relationship between the cyber architecture for ensuring acceptable frequency response and the AGC architecture of today. We highlight and confirm how the complexity of a relevant dynamic model for frequency regulation depends on the locations and the type of disturbances, and on the electrical characteristics of the interconnected system comprising the control areas with the same boundaries. This complexity will determine the most adequate cyber architecture. We stress that as the industry undergoes both technological and organizational changes, it is going to become difficult to break down a complex interconnected system into weakly connected sub-systems which would lend themselves to uncoordinated frequency regulation. For example, a Control Area (CA) with lots of wind power and very few fast-responding power plants may need to rely on power sent by other areas which have this type of plant. Provided this is done, the cost of regulating frequency at the interconnection level as a whole will be lower than without coordination. Examples of such sharing of resources across control areas already exist and are known as dynamic scheduling. A hydro power plant in CA_2 may provide regulation to the CA_1, for example. This all leads to the observation that a dynamic model relevant for the effective frequency regulation of a given interconnected system, independent of how it is partitioned, must represent the relative importance of dynamic power imbalance interactions. It is with this in mind that we formally define the notion of a dynamic interaction variable for each SBA. We show that this variable is driven by the disturbances internal to the SBA, and by the disturbances from the rest of the system as seen by the SBA model.

In the closing Section 10 we point out that the case of enhanced AGC described in this chapter is only an illustration of the enormous need to rethink what AGC is and what it might become in future electric energy systems. While much effort has been made toward major breakthroughs in the fundamental science of energy processing, it is important to recognize the huge opportunities for the enhanced utilization of energy resources presented to us by the soft technologies of sensing, communications, computing and control. These opportunities are clear but not very tangible at present in part because of the major lack of viewing the cyber design of energy systems with a full understanding of the physical characteristics of these systems, and of their temporal, spatial and contextual structures. We hope to illustrate the enormous importance of relating the physical understanding of the systems problem at hand, the models used, and the implications of these on the type of cyber required. Conversely, the models are also cyber-dependent and the recent progress in cyber technologies for power systems has opened the doors wide to progress in this area. We have attempted with great pleasure and honor to discuss the technical problem of interest, keeping in mind the early work of Joe Chow which paved our way.

2 A Dynamic Model of Electric Energy Systems with Persistent Disturbances

In this section, the general frequency dynamics model for interconnected power systems is reviewed. We assume that only generators contribute to the frequency dynamics, and we propose a module-based approach with which to establish the dynamic model, which should interconnect the generator modules and the loads with the transmission network constraints. Persistent disturbances in the system are usually caused by variable loads and renewable power sources. In this chapter, we denote the loads to be the sources of disturbances from a general point of view, in which the general loads include both the regular positive loads and the renewable power sources as negative loads.

2.1 Modeling of Generator Module

By introducing the generator module for frequency dynamics, we assume that the effects of reactive power and voltage change can be ignored and focus only on the governor-turbine model which is real-power related. In addition, in the governor-turbine model, we assume that the primary control loop has already been designed and fixed as part of the module. Recall that our purpose is to propose a secondary level control approach so that the control variable is pre-defined as the set-point of the primary control loop.

The continuous-time individual generator module with closed-loop primary control is modeled as follows [1]:

$$\begin{bmatrix} \Delta\dot{\delta}_G \\ \Delta\dot{f}_G \\ \Delta\dot{P}_T \\ \Delta\dot{a} \end{bmatrix} = \begin{bmatrix} 0 & \omega_0 & 0 & 0 \\ 0 & -\frac{D}{M} & \frac{1}{M} & \frac{e_t}{M} \\ 0 & 0 & -\frac{1}{T_t} & \frac{K_t}{T_t} \\ 0 & -\frac{1}{T_g} & 0 & -\frac{r}{T_g} \end{bmatrix} \begin{bmatrix} \Delta\delta_G \\ \Delta f_G \\ \Delta P_T \\ \Delta a \end{bmatrix} + \begin{bmatrix} 0 \\ 0 \\ 0 \\ \frac{1}{T_g} \end{bmatrix} \Delta f_G^{ref} + \begin{bmatrix} 0 \\ -\frac{1}{M} \\ 0 \\ 0 \end{bmatrix} \Delta P_G, \quad (1)$$

where the state variables $\Delta\delta_G$, Δf_G, ΔP_T and Δa correspond to the voltage phase angle deviation on the generator bus, the frequency deviation on the generator bus, the deviation of the turbine mechanical power output and the incremental change of the steam valve position, respectively. Δf_G^{ref} is the governor set-point adjustment which will be used as the control on the secondary level. ΔP_G refers to the electrical power output of the generator. ω_0 is the rated angular velocity (120π in the US power systems). M, D, T_g and T_t stand for the inertia constant of the generator, its damping coefficient and the time constants of the governor and turbine, respectively. K_t, e_t are the constant parameters of the governor-turbine primary control loop. r is defined so that $\frac{1}{r}$ is the generator speed droop.

For the ith generator module, we denote the state variables, the secondary control input as

$$\begin{aligned} \boldsymbol{x}_{G,i} &= [\Delta\delta_{G,i} \quad \Delta f_{G,i} \quad \Delta P_{T,i} \quad \Delta a_i] \\ u_{G,i} &= \Delta f_{G,i}^{ref}, \end{aligned}$$

and the module matrices as

$$\boldsymbol{A}_{G,i} = \begin{bmatrix} 0 & \omega_0 & 0 & 0 \\ 0 & -\frac{D_i}{M_i} & \frac{1}{M_i} & \frac{e_{t,i}}{M_i} \\ 0 & 0 & -\frac{1}{T_{t,i}} & \frac{K_{t,i}}{T_{t,i}} \\ 0 & -\frac{1}{T_{g,i}} & 0 & -\frac{r_i}{T_{g,i}} \end{bmatrix}, \boldsymbol{B}_{G,i} = \begin{bmatrix} 0 \\ 0 \\ 0 \\ \frac{1}{T_{g,i}} \end{bmatrix}, \boldsymbol{F}_{G,i} = \begin{bmatrix} 0 \\ -\frac{1}{M_i} \\ 0 \\ 0 \end{bmatrix}.$$

The generator module can then be represented in the state-space form:

$$\dot{\boldsymbol{x}}_{G,i} = \boldsymbol{A}_{G,i}\boldsymbol{x}_{G,i} + \boldsymbol{B}_{G,i}u_{G,i} + \boldsymbol{F}_{G,i}\Delta P_{G,i} \quad (2)$$

2.2 Modeling of the Variable Load

For the purposes of designing a dynamic model for frequency regulation, it is assumed that the load is a constant with a forecasted real power of $\boldsymbol{P}_L(0)$. Deviations of load power around its forecast $\Delta\boldsymbol{P}_L(t)$ create a disturbance in the dynamics of the interconnected power system. One can consider $\Delta\boldsymbol{P}_L(t)$ to be either a hard-to-predict deviation in demand and/or a hard-to-predict deviations in the renewable source located at the load bus. Note that the renewable power sources are defined as negative variable loads which inject randomly disturbed power into the grid. Therefore, the actual load $\boldsymbol{P}_L(t)$ can be represented as

$$\boldsymbol{P}_L(t) = \boldsymbol{P}_L(0) + \Delta\boldsymbol{P}_L(t) \tag{3}$$

2.3 Modeling of the Transmission Network Constraints

Both the dynamics of generators and load deviations are subject to transmission network constraints. The network constraints are typically expressed in terms of nodal-type algebra equations. When modules get interconnected through a transmission network the basic Kirchhoff's laws have to be satisfied. Let $\boldsymbol{S} = \boldsymbol{P} + \boldsymbol{jQ}$ be the vector of the net complex power injections to all the buses; the algebraic complex power flow equation can be written as [1]

$$\boldsymbol{S} = \mathrm{diag}(\boldsymbol{V})(\boldsymbol{Y}_{bus}\boldsymbol{V})^*, \tag{4}$$

where $\mathrm{diag}(\cdot)$ stands for the diagonal matrix with each element of the vector as a diagonal element. $\boldsymbol{V}$ is the vector of all the bus voltage phasors. The k^{th} element of $\boldsymbol{V}$ is given by $V_k e^{j\delta_{G,k}}$. $\boldsymbol{Y}_{bus}$ is the admittance matrix of the power grid.

The real part of complex power $\boldsymbol{S}$, in general, is comprised of active power injection of the generator buses $\boldsymbol{P}_G$ and consumption of the load buses $\boldsymbol{P}_L$, which is $\boldsymbol{P} = \begin{bmatrix} \boldsymbol{P}_G & -\boldsymbol{P}_L \end{bmatrix}^T$. Linearizing the real part of the complex power flow equation (4) around the operating point yields:

$$\Delta\boldsymbol{P}_G = \boldsymbol{J}_{GG}\Delta\boldsymbol{\delta}_G + \boldsymbol{J}_{GL}\Delta\boldsymbol{\delta}_L \tag{5a}$$

$$-\Delta\boldsymbol{P}_L = \boldsymbol{J}_{GL}\Delta\boldsymbol{\delta}_G + \boldsymbol{J}_{LL}\Delta\boldsymbol{\delta}_L, \tag{5b}$$

where

$$\boldsymbol{J}_{ij} = \left.\frac{\partial\boldsymbol{P}_i}{\partial\boldsymbol{\delta}_j}\right|_{\boldsymbol{\delta}_j=\boldsymbol{\delta}_j^*}, \quad \boldsymbol{i},\boldsymbol{j} \in \{G, L\}$$

are the Jacobian matrices evaluated at the given operating point. $\Delta\boldsymbol{\delta}_L$ stands for the phase angle deviations on the load buses. Assuming that $\boldsymbol{J}_{LL}$ is invertible under normal operating conditions, we can substitute $\Delta\boldsymbol{\delta}_L$ from (5b) to (5a) and obtain the system-level algebraic network coupling equation:

$$\Delta \boldsymbol{P}_G = \boldsymbol{K}_p \Delta \boldsymbol{\delta}_G + \boldsymbol{D}_p \Delta \boldsymbol{P}_L, \tag{6}$$

where

$$\begin{aligned} \boldsymbol{K}_p &= \boldsymbol{J}_{GG} - \boldsymbol{J}_{GL} \boldsymbol{J}_{LL}^{-1} \boldsymbol{J}_{LG} \\ \boldsymbol{D}_p &= -\boldsymbol{J}_{GL} \boldsymbol{J}_{LL}^{-1}. \end{aligned}$$

2.4 Modeling of the Interconnected System

The dynamic model of the interconnected system with n generators is composed of the individual generator module $\boldsymbol{x}_{G,i}$, $i = 1, 2, ..., n$ and the network constraints (6). The system-level state variables and secondary control inputs are:

$$\begin{aligned} \boldsymbol{x} &= [\boldsymbol{x}_{G,1}, \boldsymbol{x}_{G,2}, ... \boldsymbol{x}_{G,n}]^T \\ \boldsymbol{u} &= [u_{G,1}, u_{G,2}, ... u_{G,n}]^T, \end{aligned}$$

and the interconnection-removed system matrices $\boldsymbol{A}_{uc}$, $\boldsymbol{B}_{uc}$ and $\boldsymbol{F}_{uc}$ are established by locating the $\boldsymbol{A}_{G,i}, \boldsymbol{F}_{G,i}$ and $\boldsymbol{B}_{G,i}$ of each generator module on the diagonal of the matrices, respectively, which gives:

$$\begin{aligned} \boldsymbol{A}_{uc} &= \text{blockdiag}\left(\boldsymbol{A}_{G,1}, \boldsymbol{A}_{G,2}, ... \boldsymbol{A}_{G,n}\right) \\ \boldsymbol{B}_{uc} &= \text{blockdiag}\left(\boldsymbol{B}_{G,1}, \boldsymbol{B}_{G,2}, ... \boldsymbol{B}_{G,n}\right) \\ \boldsymbol{F}_{uc} &= \text{blockdiag}\left(\boldsymbol{F}_{G,1}, \boldsymbol{F}_{G,2}, ... \boldsymbol{F}_{G,n}\right). \end{aligned}$$

The system-level model will then become:

$$\dot{\boldsymbol{x}} = \boldsymbol{A}_{uc} \boldsymbol{x} + \boldsymbol{B}_{uc} \boldsymbol{u} + \boldsymbol{F}_{uc} \Delta \boldsymbol{P}_G. \tag{7}$$

We define selection matrix $\boldsymbol{S}$ such that

$$\Delta \boldsymbol{\delta}_G = \boldsymbol{S} \boldsymbol{x}, \tag{8}$$

and it can be substituted into the network constraint equation (6), which yields:

$$\Delta \boldsymbol{P}_G = \boldsymbol{K}_p \boldsymbol{S} \boldsymbol{x} + \boldsymbol{D}_p \Delta \boldsymbol{P}_L. \tag{9}$$

The full state-space model with the modules explicitly connected is then represented by combining (9) into (7):

$$\dot{\boldsymbol{x}} = \boldsymbol{A} \boldsymbol{x} + \boldsymbol{B} \boldsymbol{u} + \boldsymbol{F} \boldsymbol{w} \tag{10a}$$

$$\boldsymbol{y} = \boldsymbol{C} \boldsymbol{x}, \tag{10b}$$

where

$$\begin{aligned}
\boldsymbol{A} &= \boldsymbol{A}_{uc} + \boldsymbol{F}_{uc}\boldsymbol{K}_p\boldsymbol{S} \\
\boldsymbol{B} &= \boldsymbol{B}_{uc} \\
\boldsymbol{F} &= \boldsymbol{F}_{uc}\boldsymbol{D}_p \\
\boldsymbol{w} &= \Delta\boldsymbol{P}_L.
\end{aligned}$$

Note that the load deviations $\Delta\boldsymbol{P}_L$ are pre-defined as disturbances to the system. The deviations of variable loads and renewable power sources from their pre-scheduled values are considered as system disturbances and are both included in $\boldsymbol{w}$. In addition, since no slack generator bus is specified and removed from the state space model 10, the system matrix $\boldsymbol{A}$ is structurally singular with $rank(\boldsymbol{A}) = 4n - 1$.

3 A New Interaction Variable-Based Dynamic Model for Frequency Regulation in Large Interconnected Electric Energy Systems

The interconnected power system model (10) introduced in Section 2 may be overly complex and not necessary when designing a sensing, communication and control architecture for frequency regulation. Both temporal and spatial simplifications are possible. However, as the system changes and the nature of generation and load changes, one must proceed very carefully with such simplifications. A temporal simplification takes into consideration that, at the generator level, the internal states of the generator module consist of the fast states ΔP_T and Δa and the slow states $\Delta\delta_G$ and Δf_G. The spatial simplification mainly considers that, at the system level, the structurally singular matrix $\boldsymbol{A}$ leads to the slow dynamics which can represent the entire system's response to persistent disturbances. We address both the component and system-level time-scale separations in this section by respectively using the standard and non-standard singular perturbation form model, which had its origin in the early work of Joe Chow and his collaborators [2, 3].

The concept of an interaction variable, which is crucial to this chapter, is proposed on the basis of the non-standard form singular perturbation model. We show that the structural singularity also holds at the control area level. We introduce the definition of SBA, which refers to the control area in the new power system environment.

3.1 Standard Singular Perturbation Form-based Temporal Simplification

The standard form singular perturbation method is applied to the generator module for time-scale separation between the slow states and fast states. The standard state separable form is described by

$$\dot{\boldsymbol{x}} = \boldsymbol{f}(\boldsymbol{x},\boldsymbol{z},\boldsymbol{u},\varepsilon,t), \quad \boldsymbol{x}(t_0) = \boldsymbol{x_0}, \quad \boldsymbol{x} \in \boldsymbol{R^n} \tag{11a}$$

$$\varepsilon\dot{\boldsymbol{v}} = \boldsymbol{g}(\boldsymbol{x},\boldsymbol{v},\boldsymbol{u},\varepsilon,t), \quad \boldsymbol{v}(t_0) = \boldsymbol{v_0}, \quad \boldsymbol{v} \in \boldsymbol{R^m}, \tag{11b}$$

where $\boldsymbol{x}$ refers to the slow system states and $\boldsymbol{v}$ to the fast system states. ε is a small positive scalar which accounts for the small time constant. If the dynamics of the two states are widely separated, ε will become very small and can be approximated as $\varepsilon = 0$. This approximation is equivalent to setting the speed of $\boldsymbol{v}$ as infinitely large and the transient of $\boldsymbol{v}$ as instantaneous. Hence (11b) reduces to a set of algebra equations:

$$\boldsymbol{0} = \boldsymbol{g}(\hat{\boldsymbol{x}},\hat{\boldsymbol{v}},\hat{\boldsymbol{u}},0,t), \tag{12}$$

and the substitution of a root of (12)

$$\hat{\boldsymbol{v}} = \boldsymbol{\phi}(\hat{\boldsymbol{x}},\hat{\boldsymbol{u}},t), \tag{13}$$

into (11a) yields a reduced model:

$$\frac{d\hat{\boldsymbol{x}}}{dt} = \boldsymbol{f}(\hat{\boldsymbol{x}},\boldsymbol{\phi}(\hat{\boldsymbol{x}},\hat{\boldsymbol{u}},t),\hat{\boldsymbol{u}},0,t), \quad \hat{\boldsymbol{x}}(t_0) = \boldsymbol{x}_0, \quad \hat{\boldsymbol{x}} \in \boldsymbol{R^n}, \tag{14}$$

where the upper hat is used to indicate that the variables belong to a system with $\varepsilon = 0$. The singularly perturbed model of (2) can be obtained as

$$\frac{d\hat{\boldsymbol{x}}_{G,i}}{dt} = \hat{\boldsymbol{A}}_{G,i}\hat{\boldsymbol{x}}_{G,i} + \hat{\boldsymbol{B}}_{G,i}\hat{u}_{G,i} + \hat{\boldsymbol{F}}_{G,i}\Delta\hat{P}_{G,i}, \tag{15}$$

where

$$\begin{aligned} \hat{\boldsymbol{x}}_{G,i} &= [\Delta\delta_{G,i} \quad \Delta f_{G,i}] \\ \hat{u}_{G,i} &= \Delta f_{G,i}^{ref}, \end{aligned}$$

and

$$\hat{\boldsymbol{A}}_{G,i} = \begin{bmatrix} 0 & \omega_0 \\ 0 & -\frac{r_iD_i+K_{t,i}+e_{t,i}}{r_iM_i} \end{bmatrix}, \hat{\boldsymbol{B}}_{G,i} = \begin{bmatrix} 0 \\ \frac{K_{t,i}+e_{t,i}}{r_iM_i} \end{bmatrix}, \hat{\boldsymbol{F}}_{G,i} = \begin{bmatrix} 0 \\ -\frac{1}{M_i} \end{bmatrix}.$$

For the purposes of establishing a temporally simplified interconnected system model, we simply follow the approach in Section 2.4, and the model can be obtained as

$$\frac{d\hat{\boldsymbol{x}}}{dt} = \hat{\boldsymbol{A}}\hat{\boldsymbol{x}} + \hat{\boldsymbol{B}}\hat{\boldsymbol{u}} + \hat{\boldsymbol{F}}\hat{\boldsymbol{w}} \tag{16a}$$

$$\hat{\boldsymbol{y}} = \hat{\boldsymbol{C}}\hat{\boldsymbol{x}}, \tag{16b}$$

3.2 Non-standard Singular Perturbation Form-based Spatial Simplification

It is worthy to note that in the reduced system dynamic model (16), the structural singularity still holds, with $rank(\hat{\boldsymbol{A}}) = 2n-1$. Therefore, the dimension of the null-space $\mathscr{N}$ of $\hat{\boldsymbol{A}}$ is 1. A time-scale separation based on the non-standard singular perturbation form exists and, according to [3], the slow variable z can be obtained with the help of an $1 \times 2n$ vector $\hat{\boldsymbol{T}}$ which spans the left null-space of $\hat{\boldsymbol{A}}$, that is, $\hat{\boldsymbol{T}}\hat{\boldsymbol{A}} = 0$. Then in the reduced system model (16a), we multiply $\hat{\boldsymbol{T}}$ on both sides and it yields:

$$\frac{d\hat{z}}{dt} = \hat{\boldsymbol{T}}\frac{d\hat{\boldsymbol{x}}}{dt} = \hat{\boldsymbol{T}}\hat{\boldsymbol{B}}\hat{\boldsymbol{u}} + \hat{\boldsymbol{T}}\hat{\boldsymbol{F}}\hat{\boldsymbol{w}}, \tag{17}$$

which implies that the time response of the slow variable $\hat{z}$ only depends on the control input and the disturbances. When no control is implemented, $\hat{z}$ represents the response of the system to disturbances. The dynamics of $\hat{z}$ correspond to the zero eigenvalue of $\hat{\boldsymbol{A}}$ so we conclude that, unless an external controller is carefully designed and implemented, the system will be unable to suppress the $\hat{z}$ on its own. This also points out the necessity for secondary level frequency control: with only the locally-designed primary controller on the governor-turbine, the frequency of the power system exposed to persistent disturbances will never return to 60 Hz because of the existence of the structural singularity and the zero eigenmode.

3.3 Modeling of the Subsystem and Interaction Variable

Motivated by today's AGC approach, we extend the temporally and spatially simplified model to the subsystem level. The subsystem in today's AGC approach is denoted as the control area. Later in this subsection, we will introduce the dynamic model and a new notion to the subsystem.

The subsystem is equivalent to a stand-alone power system with external interconnections added. So it can be modeled similarly to (16) with the subscript a to differentiate it from (16),

$$\begin{aligned}\frac{d\hat{\boldsymbol{x}}_a}{dt} &= \hat{\boldsymbol{A}}_a\hat{\boldsymbol{x}}_a + \hat{\boldsymbol{B}}_a\hat{\boldsymbol{u}}_a + \hat{\boldsymbol{F}}_{a_{uc}}\hat{\boldsymbol{D}}_{p_a}\Delta\hat{P}_{L_a} + \hat{\boldsymbol{F}}_{a_{uc}}\hat{\boldsymbol{D}}_{p_a}\Delta\hat{F}_{L_a} - \hat{\boldsymbol{F}}_{a_{uc}}\Delta\hat{F}_{G_a} \\ &= \hat{\boldsymbol{A}}_a\hat{\boldsymbol{x}}_a + \hat{\boldsymbol{B}}_a\hat{\boldsymbol{u}}_a + \hat{\boldsymbol{F}}_a\hat{\boldsymbol{w}}_a, \end{aligned} \tag{18}$$

where

$$
\begin{aligned}
\hat{\boldsymbol{F}}_a &= \begin{bmatrix} \hat{\boldsymbol{F}}_{a_{uc}} \hat{\boldsymbol{D}}_{p_a} & \hat{\boldsymbol{F}}_{a_{uc}} \hat{\boldsymbol{D}}_{p_a} & -\hat{\boldsymbol{F}}_{a_{uc}} \end{bmatrix} \\
\hat{\boldsymbol{w}}_a &= \begin{bmatrix} \Delta \hat{P}_{L_a} \\ \Delta \hat{F}_{L_a} \\ \Delta \hat{F}_{G_a} \end{bmatrix}.
\end{aligned} \tag{19}
$$

The term $\Delta \hat{F}_{G_a}$ stands for the power flow from the neighboring control areas to the generator buses, and $\Delta \hat{F}_{L_a}$ is the power flow from the neighboring control areas to the load buses. Hence, at the control area level, disturbances to a control area could be from its own loads and/or the tie-lines connecting to other areas.

Structural singularity also exists in (18), so we can apply the non-standard form singular perturbation method to the subsystem model as in Section 3.2, which leads to

$$
\frac{d\hat{z}_a}{dt} = \hat{\boldsymbol{T}}_a \frac{d\hat{\boldsymbol{x}}_a}{dt} = \hat{\boldsymbol{T}}_a \hat{\boldsymbol{B}}_a \hat{\boldsymbol{u}}_a + \hat{\boldsymbol{T}}_a \hat{\boldsymbol{F}}_a \hat{\boldsymbol{w}}_a. \tag{20}
$$

The dynamics of the slow variable $\hat{z}_a$ depend solely on the internal control input and the disturbances from internal and external energy sources. When no internal control is applied, $\hat{z}_a$ represents the interaction of the subsystem to the imbalances caused by the internal and external disturbances.

We propose the notion of an Interaction Variable [1] to the slow variable $\hat{z}_a$ and define it as

Definition 1. The interaction variable $\hat{z}_a$ of a control area is the variable that satisfies

$$
\frac{d\hat{z}_a}{dt} \equiv 0,
$$

when no control input is applied, no internal disturbance is imposed and all interconnections with other control areas are removed.

As in Section 3.2, the interaction variable $\hat{z}_a$ is an aggregation of the state variables of a control area, namely,

$$
\hat{z}_a = \hat{\boldsymbol{T}}_a \hat{\boldsymbol{x}}_a, \tag{21}
$$

and $\hat{\boldsymbol{T}}_a$ is the basis of the eigenspace $\mathscr{N}(\hat{\boldsymbol{A}}_a)$ and can be determined by solving

$$
\hat{\boldsymbol{T}}_a \hat{\boldsymbol{A}}_a = 0. \tag{22}
$$

Denote $\hat{z}_a$ as the output variable of the subsystem and write the subsystem model as

$$
\frac{d\hat{\boldsymbol{x}}_a}{dt} = \hat{\boldsymbol{A}}_a \hat{\boldsymbol{x}}_a + \hat{\boldsymbol{B}}_a \hat{\boldsymbol{u}}_a + \hat{\boldsymbol{F}}_a \hat{\boldsymbol{w}}_a \tag{23a}
$$

$$
\hat{z}_a = \hat{\boldsymbol{C}}_a \hat{\boldsymbol{x}}_a, \tag{23b}
$$

where

$$\hat{\boldsymbol{C}}_a = \hat{\boldsymbol{T}}_a.$$

At the end of this section, we define a new notion of Smart Singular Authority (SBA) as the control area (subsystem) which communicates its interaction variable with the rest of the system in order to balance supply and demand on real time by relying on-line adjustments of the resources internal to the subsystem and the neighboring subsystems. Both the concepts of interaction variable and SBA will be used in the future sections for designing the cyber architecture of the frequency regulation system.

4 Interaction Variable-Based Dynamical Models for Frequency Regulation: Comparison of Model Complexity for Four Qualitatively Different Cases

In this section, we illustrate the role of the interaction variables in four qualitatively different systems. The 5-bus power system shown in Figure 1 is used to demonstrate the four different scenarios without loss of generality. The pre-defined organizational boundaries divide the system into two interconnected subsystems (SBAs). However, as the internal and external electrical distances and disturbances change qualitatively, the dynamic interaction between these two SBAs can differ dramatically. Tables 1 and 2 list the system parameters and $\hat{\boldsymbol{A}}$ matrices, respectively. In this section we basically assume that the magnitude and rate of change of the disturbances stay within a pre-specified range so that the cases with different electrical distances can be addressed with emphasis.

Table 1 Parameters of the 5-bus test system ($S_{base} = 100MVA$)

Transmission Line Reactance Data (p.u.)							
	X_{12}	X_{14}	X_{23}	X_{24}	X_{35}	X_{45}	
Case 1	0.01	0.01	20	0.01	0.01	20	
Case 2	1	1	20	1	1	20	
Case 3	0.01	0.01	0.01	0.01	0.01	0.01	
Case 4	1	1	0.01	1	1	0.01	
Generator Data (p.u.)							
	M	D	T_t	T_g	e_t	K_t	r
Gen 1	8	2	0.2	0.25	39.4	250	19
Gen 2	10	2	0.18	0.23	39.4	250	19
Gen 3	9	1.6	0.3	0.3	39	280	21

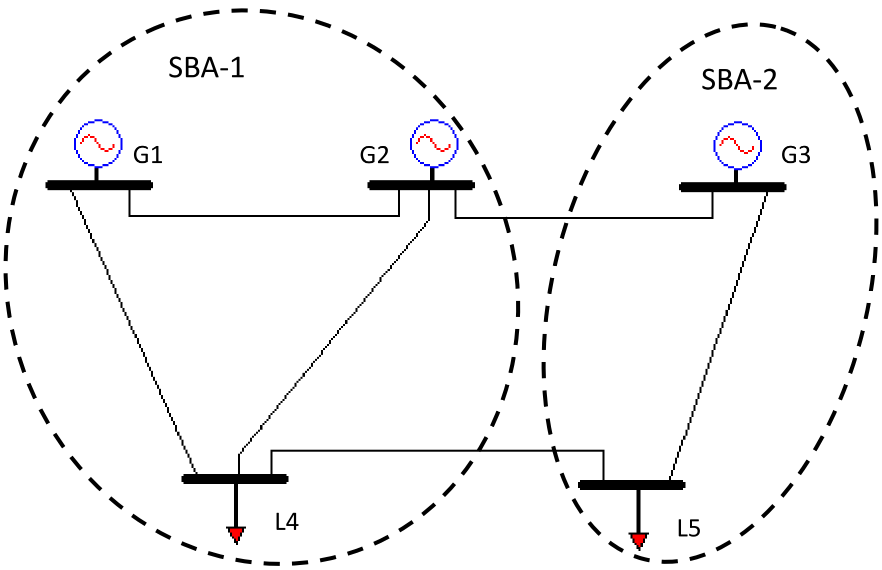

Fig. 1 5-bus power system

Table 2 System $\hat{\boldsymbol{A}}$ Matrices in the Four Cases

Case 1	Case 2
$\hat{\boldsymbol{A}} = \begin{bmatrix} 0 & 377 & 0 & 0 & 0 & 0 \\ -18.75 & -2.15 & 18.75 & 0 & 0.0031 & 0 \\ 0 & 0 & 0 & 377 & 0 & 0 \\ 15 & 0 & -15 & -1.72 & 0.0075 & \\ 0 & 0 & 0 & 0 & 0 & 377 \\ 0.0028 & 0 & 0.0083 & 0 & -0.0111 & -1.87 \end{bmatrix}$	$\hat{\boldsymbol{A}} = \begin{bmatrix} 0 & 377 & 0 & 0 & 0 & 0 \\ -0.19 & -2.15 & 0.19 & 0 & 0.0029 & 0 \\ 0 & 0 & 0 & 377 & 0 & 0 \\ 0.15 & 0 & -0.16 & -1.72 & 0.0073 & \\ 0 & 0 & 0 & 0 & 0 & 377 \\ 0.0026 & 0 & 0.0081 & 0 & -0.0107 & -1.87 \end{bmatrix}$
Case 3	Case 4
$\hat{\boldsymbol{A}} = \begin{bmatrix} 0 & 377 & 0 & 0 & 0 & 0 \\ -20 & -2.15 & 17.5 & 0 & 2.5 & 0 \\ 0 & 0 & 0 & 377 & 0 & 0 \\ 14 & 0 & -26 & -1.72 & 12 & \\ 0 & 0 & 0 & 0 & 0 & 377 \\ 2.22 & 0 & 13.33 & 0 & -15.55 & -1.87 \end{bmatrix}$	$\hat{\boldsymbol{A}} = \begin{bmatrix} 0 & 377 & 0 & 0 & 0 & 0 \\ -0.17 & -2.15 & 0.14 & 0 & 0.0345 & 0 \\ 0 & 0 & 0 & 377 & 0 & 0 \\ 0.11 & 0 & -10.13 & -1.72 & 10.02 & \\ 0 & 0 & 0 & 0 & 0 & 377 \\ 0.0307 & 0 & 11.14 & 0 & -11.17 & -1.87 \end{bmatrix}$

4.1 Cases 1 and 2

In the first case, the system has two weakly interconnected SBAs with small internal electrical distances. The system is therefore modeled using the concept of interaction variables proposed in this chapter, for which we have

$$\hat{z}_a^I \triangleq \hat{c}_{a,1}^I \hat{x}_{a,1}^I + \hat{c}_{a,2}^I \hat{x}_{a,2}^I \tag{24a}$$

$$\hat{z}_a^{II} \triangleq \hat{c}_{a,1}^{II} \hat{x}_{a,1}^{II}, \tag{24b}$$

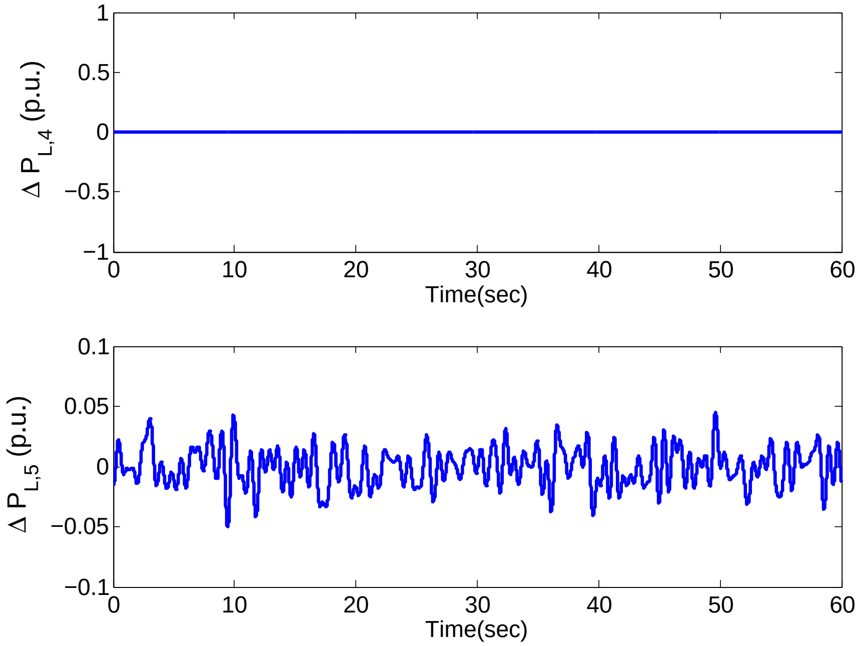

Fig. 2 Continuous real power disturbances

where $\hat{C}_a^I$ and $\hat{C}_a^{II}$ can be solved from equation (22). It is shown in Figure 3.(a) that when the system is driven by fast oscillating disturbances (depicted by Figure 2), the dynamics of the interaction variables of SBA-2 are significantly affected. By contrast, the interaction variables of SBA-1 have much slower dynamics. Note that the positive direction of the interaction variables can be arbitrarily assigned.

Case 2 represents an overall weakly connected system. The interaction variables for this case are presented in Figure 3.(b). The results resemble those of case 1 due to the fact that the dynamic behaviors of $\hat{z}_a^I$ and $\hat{z}_a^{II}$ differ significantly and SBA-1 and SBA-2 interact weakly.

We conclude that in cases 1 and 2 the dynamics of the interaction variables depend mainly on internal disturbances; and we propose that, because of the insignificant interactions between the SBAs in these cases, there is no need to dynamically exchange measurements across the SBAs in order to ensure the desired frequency quality. Instead, we could design a decentralized controller for each SBA based on its respective output measurements.

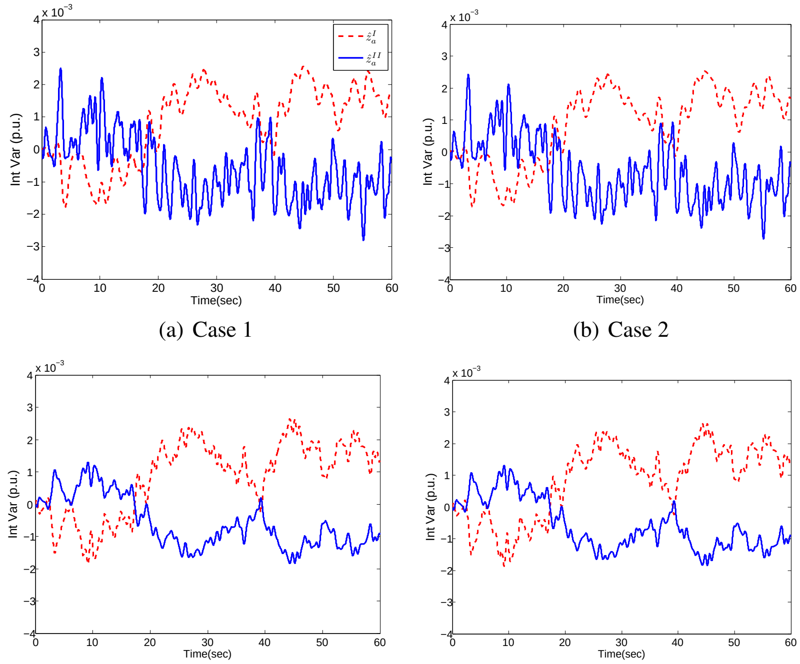

(a) Case 1 (b) Case 2

(c) Case 3 (d) Case 4

Fig. 3 Interaction Variables of the Four Qualitatively Different Cases

4.2 *Cases 3 and 4*

In this subsection we analyze two more cases which are qualitatively different from the previous cases. In case 3, the system is characterized by strong electrical connections both between and within the SBAs. In case 4 the system has strong inter-area electrical connections and weak intra-area connections. The interaction variables of SBA-1 and SBA-2 can be obtained similarly to equation (24) and demonstrated by Figure 3.(c) and (d), respectively.

In Figure 3.(c), the strong interactions between SBAs 1 and 2 in case 3 are illustrated through the highly similar behavior of the interaction variables of the SBAs. This is because the components in the system are tightly connected and the two SBAs consequently behave like one system. Figure 3.(d) shows the interaction variables of case 4, which are as strong as those of case 3. In case 4, Generator 2 is electrically much closer to SBA-2 but is organizationally grouped into SBA-1.

It is seen from the results that both $\hat{z}_a^I$ and $\hat{z}_a^{II}$ have strong dynamics even through only SBA-2 is subject to continuous disturbances. So we conclude that unless the coordination among SBAs for minimizing interaction variables is carefully designed, a decentralized CA level control will not guarantee good frequency response.

5 Coherency-Based Dynamical Models for Frequency Regulation: Comparison of Model Complexity for Four Qualitatively Different Cases

The early work by Joe Chow on slow coherency is referred to in this section [2, 4, 5, 6]. His slow coherency-based approach is used to partition the interconnected power system into weakly interconnected subsystems. This partitioning leads to the time-scale separation of slow inter-area dynamics from fast intra-area dynamics. Machines within each resulting subsystem should operate with similar motions with respect to the slow eigenmodes of the system [6]. This concept of slow coherency dynamics is similar to the concept of interaction variables in our work proposed in Section 3. We will briefly introduce the slow coherency-based approach and show how it applies to the 4-case study in the 5-bus power system.

In the linear time-invariant (LTI) system $\dot{\boldsymbol{x}} = \boldsymbol{A}\boldsymbol{x}$, states x_i and x_j are defined as σ_a-coherent, which is coherent with respect to r modes of $\boldsymbol{A}$, if and only if none of these modes is observable from

$$y_j(t) = x_j(t) - x_i(t) = c_j\boldsymbol{x}(t), \tag{25}$$

where the only nonzero entries of row c_j are its ith entry -1 and jth entry 1 [5]. So by this definition, if x_i and x_j are coherent with respect to the excited σ_a-modes, then $x_j(t) - x_i(t) = 0$. It is algebraically equivalent to identify the identical rows of an $n \times r$ matrix $\boldsymbol{V}$:

$$c_j\boldsymbol{V} = 0, \tag{26}$$

where the columns of $\boldsymbol{V}$ are the corresponding eigenvectors of the σ_a-modes. Since the rank of $\boldsymbol{V}$ is r, the smallest number of different subgroups which contain identical rows of $\boldsymbol{V}$ is r. Therefore the smallest possible number of coherent subgroups is r.

By applying the slow coherency-based approach to the 5-bus power system shown in Figure 1 for the 4-case study, the resulting weakly connected coherent subgroups for each case are demonstrated in Figure 4 respectively. To design a frequency regulation architecture for the slow coherency-partitioned system, we propose to use the decentralized state feedback controller for each subsystems based on its own state measurements with no information exchange across the subsystems because they are either weakly connected (Figure 4.(a), (b) and (d)) or stand-alone (Figure 4.(c)).

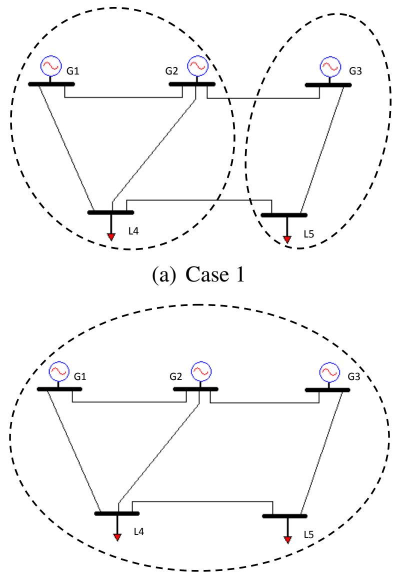

(a) Case 1 (b) Case 2

(c) Case 3 (d) Case 4

Fig. 4 Slow Coherency-based Partitioning of the Four Qualitatively Different Cases

6 Comparison of Interaction Variable-Based and Coherency-Based Dynamic Models Relevant for Frequency Regulation

It is seen from the previous sections 4 and 5 that both the interaction variable-based approach and the slow coherency-based approach can interpret the interactions between subareas and assist in the design of a modeling, sensing, control and communication system for frequency regulation. The conclusions, based on the numerical results of sections 4 and 5, which the two approaches arrive at via different paths are compared in this section. Their implications for frequency regulation system design will then be discussed based on the comparisons.

The interaction variable-based approach determines the strength of interactions among SBAs by examining the interaction variables of the SBAs. For example, in the case when the SBA has weak external but strong internal electrical connections (case 1 in Section 4 and 5), the interaction variables presented in Figure 3.(a) have a noticeable difference in dynamics with $\hat{z}_a^I$ evolving much slower than $\hat{z}_a^{II}$. The different dynamics imply a weak interaction between the two SBAs. In case 3, the interaction variables shown in Figure 3.(c) have similar dynamics to each other. This high similarity indicates a strong interaction between the two SBAs. In the other two cases, the strength of the interaction between the two SBAs can also be identified by following the same procedure.

In comparison, the slow coherency-based approach breaks the system down into weakly connected coherent subsystems (CSubs). We identify the strength of interaction between SBAs by comparing the boundaries of SBAs and the boundaries of CSubs. If the boundaries of SBAs matches the boundaries of CSubs, the interactions among the SBAs will be weak; if not, strong interactions can be identified. In case 1, Figure 1 and 4.(a) illustrate that the SBAs have the same boundary as the CSubs, so that weak interaction exist between the SBAs. In case 2, as shown in Figure 4.(b), although the SBA-1 is divided into two subgroups, the boundary of SBA-1 and SBA-2 still match the boundary of the other two CSubs, which indicates weak interactions exist inside SBA-1 and also between SBA-1 and SBA-2. In cases 3 and 4, the slow coherency-based approach tends to either group all generators into one single system (case 3) or group part of the generators in SBA-1 into SBA-2 (case 4); both cases exhibit strong interaction between SBA-1 and SBA-2.

As a result, the two approaches arrive at the same conclusion, via different paths, concerning the evaluation of the SBA interaction strength. Both approaches can assist us in the design of cyber architecture for the E-AGC system with respect to the interaction strength. In short, when the interactions among the SBAs are weak, there is no need for coordination of the SBAs. If the interactions are not weak, the SBAs will have to exchange information dynamically and be coordinated in order to ensure the global minimization of the imbalance between power supply and demand and good frequency response at the system level.

7 Two Qualitatively Different Cyber Architectures for Regulating Frequency Using Interaction Variable-Based Models

In this section, the cyber architecture of the E-AGC system is designed by employing the interaction variable-based model. According to what has been discussed in Sections 4 and 6 different control and communication architectures are needed for strong and weak interaction scenarios, respectively. In each scenario, we formulate the control design problem, using the Linear Quadratic Regulator (LQR) to ensure that the interactions among all SBAs and the control inputs are limited to acceptable levels.

7.1 Weak Interaction Scenario

In the weak interaction scenario, a decentralized linear output feedback control with no information exchange among the SBAs is designed. For the ith SBA modeled by (23), the linear output feedback control is expressed as

$$\hat{\boldsymbol{u}}_a^i = -\hat{\boldsymbol{K}}_a^i \hat{z}_a^i, \tag{27}$$

where $\hat{\boldsymbol{K}}_a^i$ is the feedback control gain vector and $\hat{z}_a^i$ is the interaction variable of the ith SBA.

We determine the proper constant gains $\hat{\boldsymbol{K}}_a^i$ by solving the following LQR-based optimization problem:

$$\begin{aligned}
\underset{\hat{\boldsymbol{u}}_a^i}{\text{minimize}} \quad & J = \frac{1}{2}\int_0^{\infty} \left[(\hat{z}_a^i)^2 q_a^i + (\hat{\boldsymbol{u}}_a^i)^T \boldsymbol{R}_a^i (\hat{\boldsymbol{u}}_a^i)\right] dt \\
\text{subject to} \quad & \frac{d\hat{\boldsymbol{x}}_a^i}{dt} = \hat{\boldsymbol{A}}_a^i \hat{\boldsymbol{x}}_a^i + \hat{\boldsymbol{B}}_a^i \hat{\boldsymbol{u}}_a^i \\
& \hat{z}_a^i = \hat{\boldsymbol{C}}_a^i \hat{\boldsymbol{x}}_a^i \\
& \hat{\boldsymbol{u}}_a^i = -\hat{\boldsymbol{K}}_a^i \hat{z}_a^i.
\end{aligned} \tag{28}$$

The non-negative scalar q_a^i in the quadratic objective function is considered to be an indicator of the willingness of the ith SBA to eliminate its own interaction variable. The positive definite matrix $\boldsymbol{R}_a^i$, on the other hand, presents how much it will cost the sources to provide the frequency regulation service.

Accordingly, the communication scheme for the entire system can be designed on the assumption that the communication channels only exist inside each SBA, which are between the control center and the generators that belong to this SBA (shown in Figure 5). Each generator measures its internal states and uploads the information to the control center, which estimates the interaction variable after gathering the measurement of all states in the area. Control signals will then be distributed back to each generator which participates in the frequency regulation service.

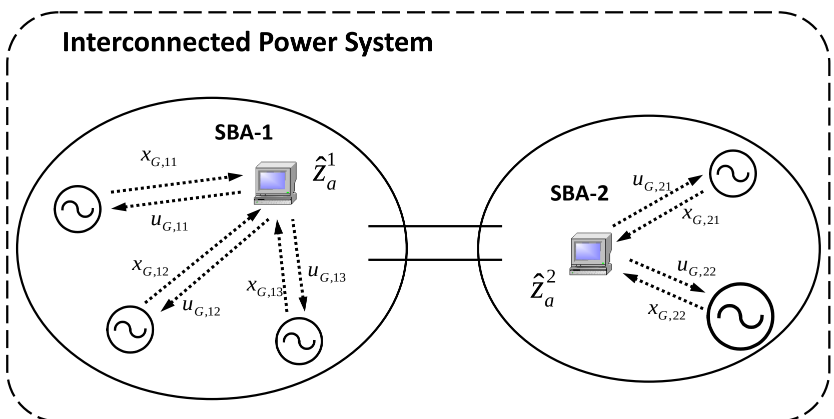

Fig. 5 The Communication Scheme of the E-AGC System in the Weak Interaction Scenario

7.2 Strong Interaction Scenario

In the strong interaction scenario, a system-level coordinated output feedback control with information dynamically exchanged among the SBAs is designed. Recalling the singularly perturbed dynamic model for the entire system (16), the linear output feedback control can be represented by

$$\hat{\boldsymbol{u}} = -\hat{\boldsymbol{K}}\hat{\boldsymbol{y}}, \tag{29}$$

where $\hat{\boldsymbol{y}}$ is a vector whose entries are the interaction variables of all SBAs; if we let N be the number of SBAs we have:

$$\begin{aligned} \hat{\boldsymbol{y}} &= \hat{\boldsymbol{C}}\hat{\boldsymbol{x}} \\ \hat{\boldsymbol{C}} &= \text{blockdiag}\left(\hat{\boldsymbol{C}}_a^1, \hat{\boldsymbol{C}}_a^2, \ldots \hat{\boldsymbol{C}}_a^N\right) \end{aligned} \tag{30}$$

For this scenario, we propose an LQR-based optimization problem to obtain the output feedback control gain matrix $\hat{\boldsymbol{K}}$, which is

$$\begin{aligned} \underset{\hat{\boldsymbol{u}}}{\text{minimize}} \quad & J = \frac{1}{2}\int_0^\infty \left[\hat{\boldsymbol{y}}^T \boldsymbol{Q}\hat{\boldsymbol{y}} + \hat{\boldsymbol{u}}^T \boldsymbol{R}\hat{\boldsymbol{u}}\right] dt \\ \text{subject to} \quad & \frac{d\hat{\boldsymbol{x}}}{dt} = \hat{\boldsymbol{A}}\hat{\boldsymbol{x}} + \hat{\boldsymbol{B}}\hat{\boldsymbol{u}} \\ & \hat{\boldsymbol{y}} = \hat{\boldsymbol{C}}\hat{\boldsymbol{x}} \\ & \hat{\boldsymbol{u}} = -\hat{\boldsymbol{K}}\hat{\boldsymbol{y}}. \end{aligned} \tag{31}$$

The positive semi-definite matrix $\boldsymbol{Q}$ is the quadratic objective function which indicates all SBAs' willingness to eliminate their own interaction variables. The positive definite matrix $\boldsymbol{R}$ stands for the cost the generators will incur in providing frequency regulation service.

Compared to the weak interaction scenario, the communication scheme in the strong interaction scenario is designed so that communication channels exist not only internally between the SBA control center and the internal generators but also among the control centers (shown in Figure 6). The SBA control center gathers the internal states information, exchanges its own interaction variable with other SBAs and distributes the control signals to the generators that contribute to the frequency regulation service.

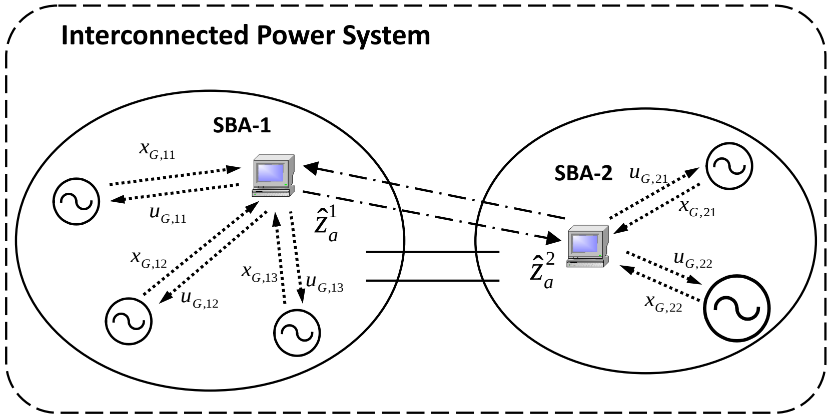

Fig. 6 The Communication Scheme of the E-AGC System in the Strong Interaction Scenario

8 Cyber Architecture for Slow Coherency-based Regulating Frequency and Comparative Simulation Study

8.1 Design of the Cyber-Architecture

This section designs the control and communication architecture of the frequency regulation system by following the slow coherency-based approach which was introduced and discussed in Sections 5 and 6. A decentralized state feedback control is proposed for each CSub separately due to the fact that all the electrical interconnections are weak among the CSubs revealed by the slow coherency-based approach, and the size of each CSub is usually relatively small, so that no much measurement and communication is needed even though the control is full state feedback-based.

The control and communication scheme is much the same as the one in Section 7.1. The only difference is that, in this section, we replace the interaction variable in the objective function with the full states of the CSub.

$$\hat{\boldsymbol{u}}_c^i = -\hat{\boldsymbol{K}}_c^i \hat{\boldsymbol{x}}_c^i \tag{32}$$

The LQR-based optimization problem can be formulated as

$$\begin{aligned} \underset{\hat{\boldsymbol{u}}_c^i}{\text{minimize}} \quad & J = \frac{1}{2}\int_0^{\infty} \left[(\hat{\boldsymbol{x}}_c^i)^T \boldsymbol{Q}_c^i \hat{\boldsymbol{x}}_c^i + (\hat{\boldsymbol{u}}_c^i)^T \boldsymbol{R}_c^i \hat{\boldsymbol{u}}_c^i \right] dt \\ \text{subject to} \quad & \frac{d\hat{\boldsymbol{x}}_c^i}{dt} = \hat{\boldsymbol{A}}_c^i \hat{\boldsymbol{x}}_c^i + \hat{\boldsymbol{B}}_c^i \hat{\boldsymbol{u}}_c^i \\ & \hat{\boldsymbol{u}}_c^i = -\hat{\boldsymbol{K}}_c^i \hat{\boldsymbol{x}}_c^i . \end{aligned} \tag{33}$$

The communication architecture is shown in Figure 7; it has information exchange only within each CSub and works quite similarly to the interaction variable-based architecture in the weak interaction scenario.

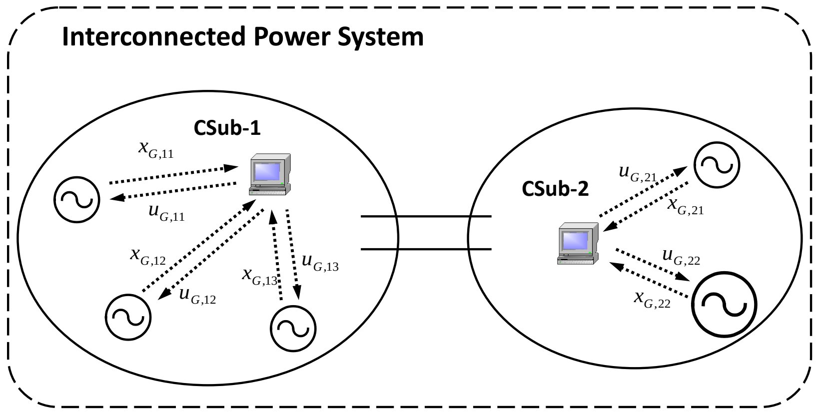

Fig. 7 The Communication Scheme of the Slow Coherency-based Frequency Regulation System

8.2 Comparative Study via Numerical Simulations

The interaction variable-based frequency regulation approach (E-AGC) proposed in Section 7 and the slow coherency-based frequency regulation approach are compared, via numerical simulations, on a 5-bus power system (Figure 1) which is exposed to the disturbances shown in Figure 2. The system performances of the four qualitatively different cases are illustrated respectively.

In Figure 8-11, the system frequency performances of the four cases are demonstrated. In the first row of each figure, the subplots correspond to the frequency of Generators 1, 2 and 3 when no regulation exists. In the second row, the subplots are for the E-AGC; in the third row, they are for the slow coherency-based approach. In Figure 12-15, the responses of the interaction variables are demonstrated for the four cases. Note that only the E-AGC defines the interaction variable and utilizes it in the feedback control design. Therefore, each figure has only two rows of subplots, in which the first row stands for no regulation and the second row represents the performance of E-AGC.

The results show that both approaches are able to effectively suppress the frequency deviation caused by the persistent disturbances. The E-AGC approach eliminates the imbalances (represented by the interaction variables in Figure 12-15) and the frequency deviations which are, in fact, a consequence of the imbalances. The slow coherency-based approach performs quite closely to the interaction variable-based E-AGC but it costs much more on communications for the state feedback controller. Besides, the CSubs' boundaries remain unfixed in the slow coherency-based approach and may vary with respect to the changes in system structure or operating equilibrium. In this case, the communication scheme for frequency regulation needs to be dynamically updated in real time, which is hard for large-scale system operations. By contrast, the interaction variable-based E-AGC system uses a predetermined boundary and communication scheme for each SBA. Changes in system structure or operating equilibrium only affect the necessity of information exchange among SBAs. We conclude that it is more applicable to design an interaction variable-based E-AGC for frequency regulation.

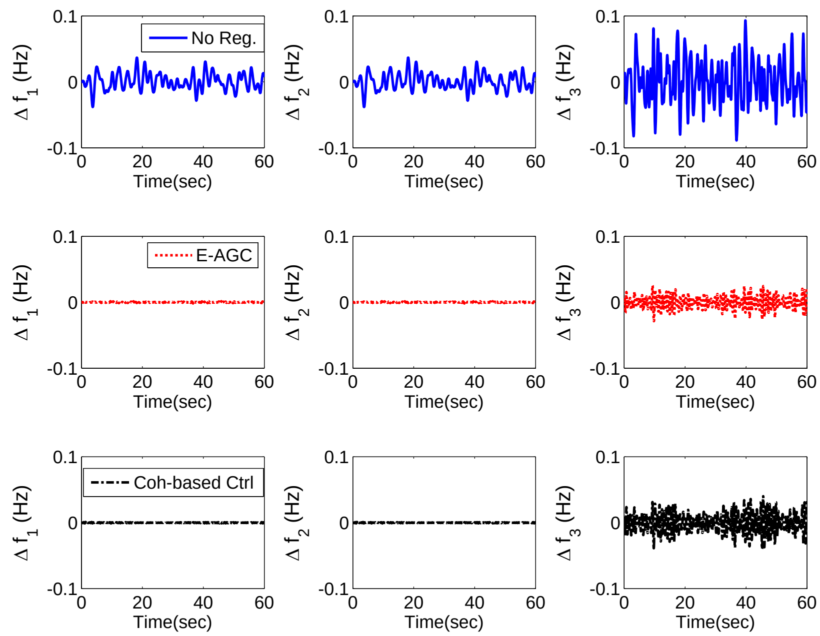

Fig. 8 System Frequency Performance for Case 1

9 Comparison of the E-AGC and Today's AGC

This section compares the proposed E-AGC approach and today's AGC approach. We first recall the current state of the ACE in today's AGC system. The linear combination of area-wide frequency deviation and net tie-line flow is defined as the ACE to represent the area-wide real power imbalance. The ingenious aspect of ACE is that for a control area which is free of disturbances, the corresponding ACE will

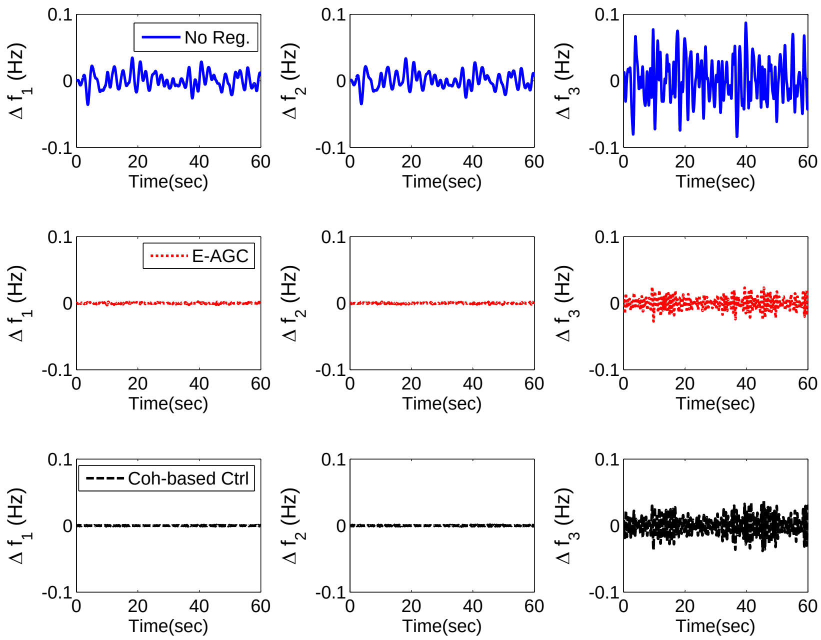

Fig. 9 System Frequency Performance for Case 2

be zero. In other words, only the control areas exposed to disturbance sources have non-zero ACEs. Consequently, by using ACE to feed into the PI-based secondary controller, each control area responses only to its own imbalance. And as long as all control areas compensate for their ACEs, the imbalances of the entire system will be eliminated and the frequency and net tie-line flow will be regulated. The ACE-based AGC scheme is fully decentralized with no need for information exchange among the control areas since both the net tie-line flow and frequency deviations are measurable at the control area level.

However, the ACE-based AGC scheme is not optimally designed. Firstly, it assumes a perfect estimation of the frequency bias, which is hard to achieve practically. Secondly, from the perspective of cost-effectiveness, the implementation of ACE initially blocks the opportunity for systematically utilizing cheap and fast resources in frequency regulation. For example, if one control area is subjected to a large amount of fast disturbances and its resources for frequency regulation are either too expensive or too slow, the ACE-based AGC has no choice but to use these resources and pay much more for them rather than to import service from much cheaper and faster resources belonging to other control areas.

The potential advantages of applying the E-AGC are pointed out and discussed in the following:

- The E-AGC accounts for the SBA's requisition on the magnitude of imbalance and the capability of participating in frequency regulation service. And it pro-

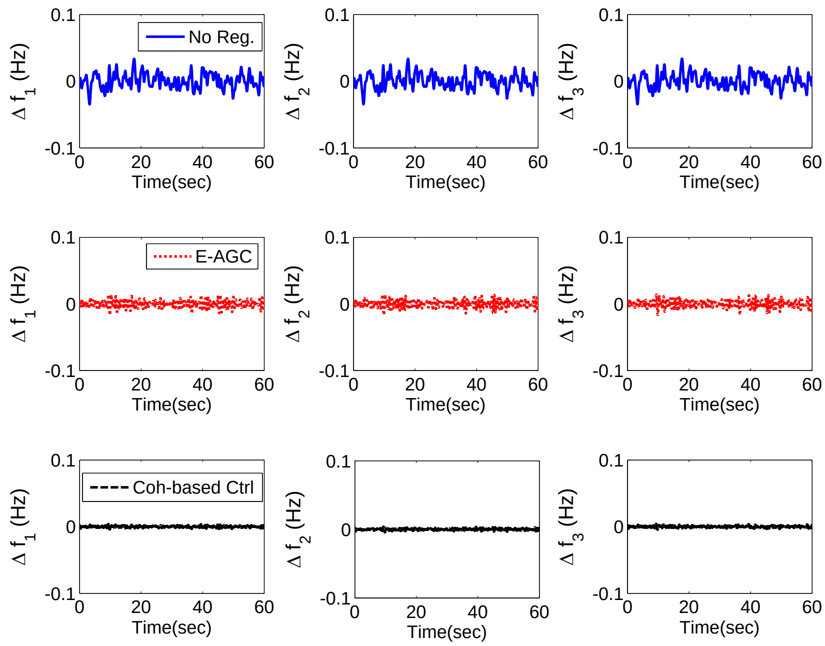

Fig. 10 System Frequency Performance for Case 3

vides an opportunity to the SBAs equipped with cheap and fast frequency regulation dedicated generating units to provide service to other SBAs and improve the cost-effectiveness of the frequency regulation service of the entire system. However, in contrast to the E-AGC, the ACE-based AGC of each control area only regulates its own imbalance, which does not translate automatically to a systematic cost-effectiveness of the frequency regulation service.

- The amount of exchanged information is limited. The interaction variable is the only information that each SBA needs to share with the rest of the system. This indicates a significant savings on investment and on maintenance for the communication system. In contrast, for the normally-used LQR-based state feedback control architecture, the full system states need to be measured, and either gathered in a centralized control center or exchanged with all other areas. So state feedback control is impractical in relatively large-scale power systems because too much communication is required. Large amounts of communication will result in both high costs and a high probability of congestion in communications channels, which will result in a deterioration of control performance.
- The role of Phasor Measurement Units (PMUs) is profound. In the proposed E-AGC approach, the deployment of PMUs is necessary because, as in (21), the SBA needs to measure its internal state variables; these include the generator voltage phase angles. Only PMUs can provide fast and highly accurate measurements of the voltage phase angles. In addition, the differences between fre-

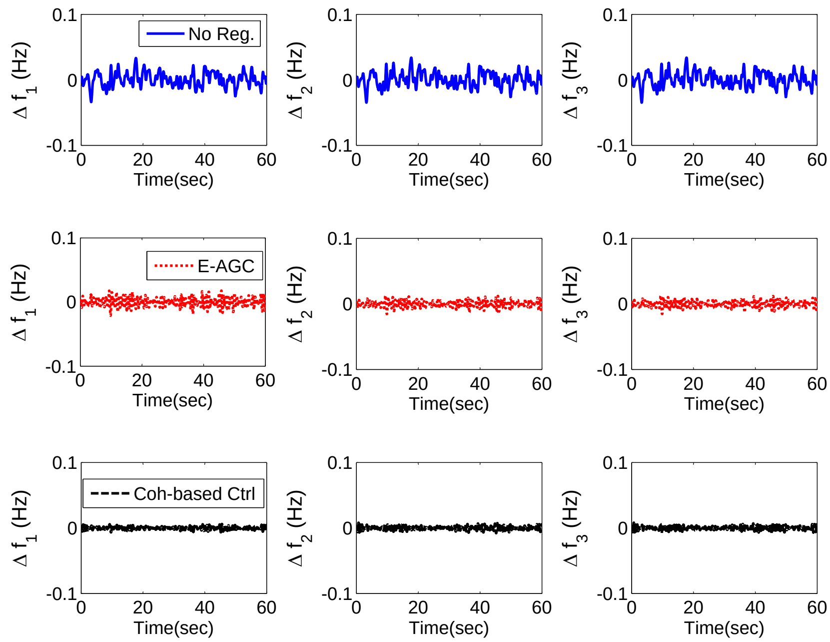

Fig. 11 System Frequency Performance for Case 4

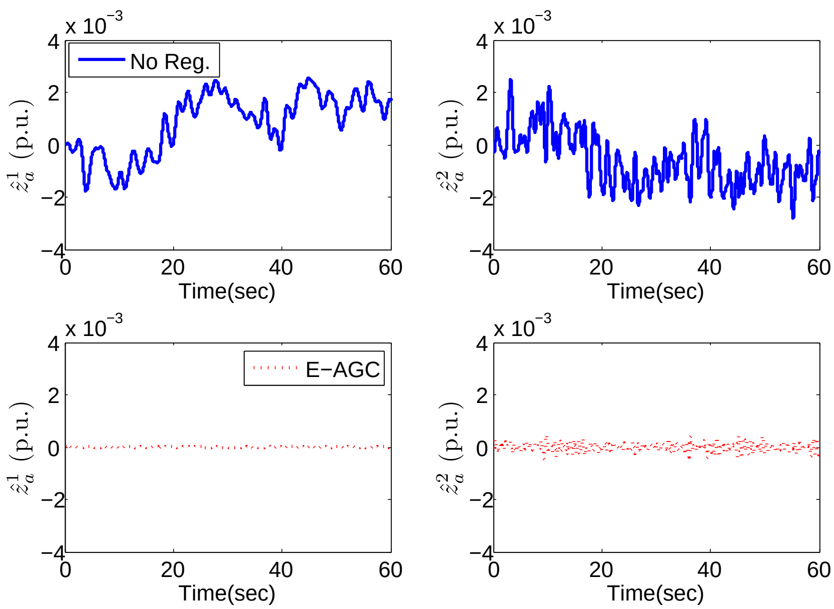

Fig. 12 System Interaction Variable Performance for Case 1

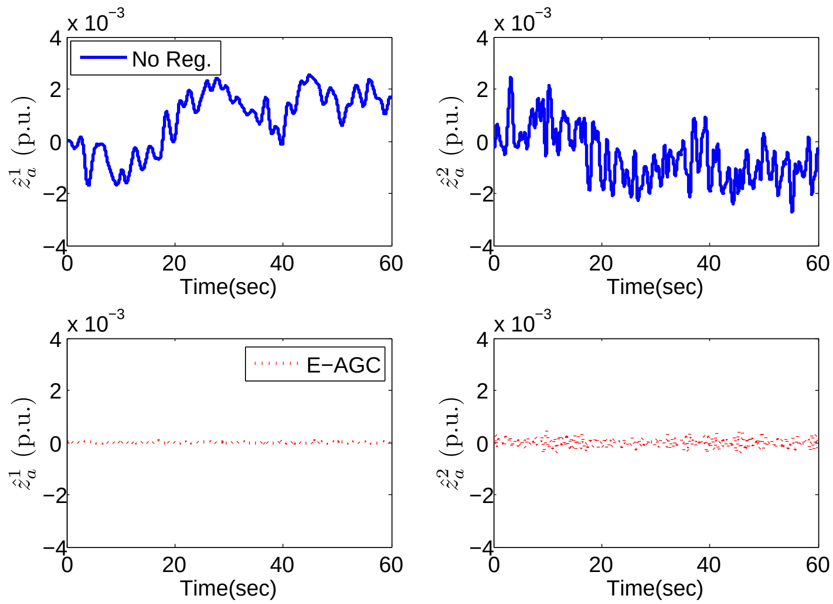

Fig. 13 System Interaction Variable Performance for Case 2

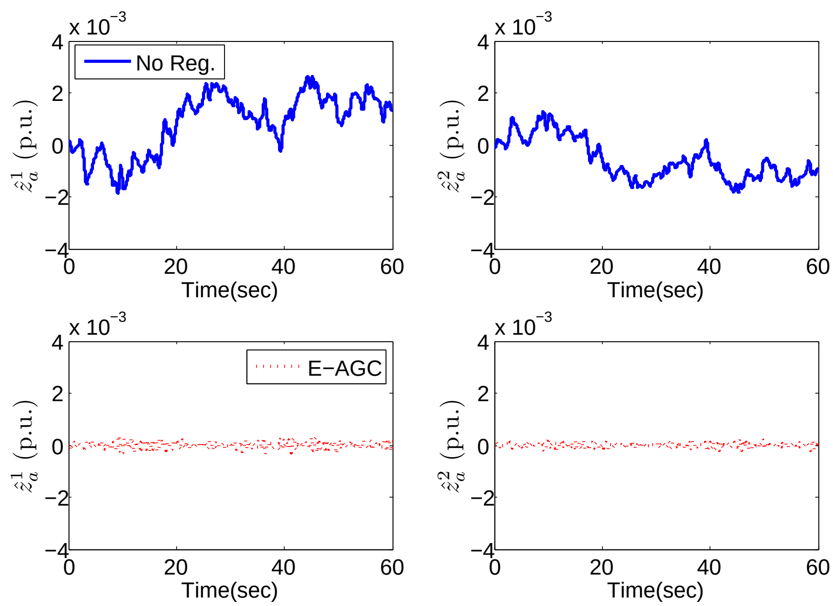

Fig. 14 System Interaction Variable Performance for Case 3

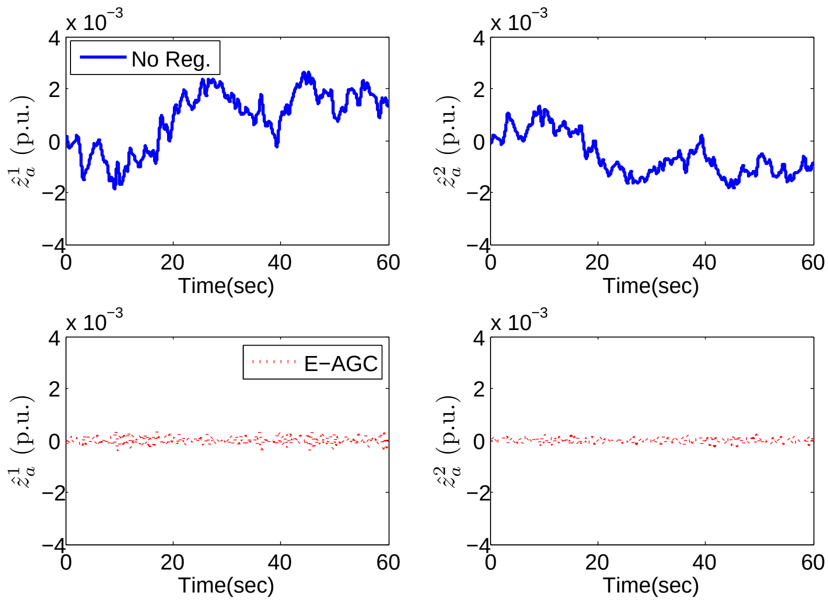

Fig. 15 System Interaction Variable Performance for Case 4

quencies on different generator buses inside the SBA can only be distinguished by high-accuracy and high-resolution devices like PMUs. Therefore, in order to have a correct estimation of the interaction variable for the SBA, sufficient PMUs have to be deployed.

- The use of interaction variables as interchanged information also protects the privacy of each SBA. Since the $\hat{C}_a^i$ for the SBA is not an invertible matrix but a vector, the other SBAs, as long as they have no complete knowledge of the structure and components of this SBA, cannot extract its information about the states from the interaction variable.

10 Open Questions and Future Work

In this chapter we rethink the balancing of hard-to-predict supply and demand variations around their forecast by using frequency regulation in future electric energy systems. We conclude that the design of sensing, communication and control architectures requires a clear understanding of the temporal and spatial characteristics of the power grid as well as of its generation and load dynamics. We propose an E-AGC which would fulfill these requirements. Modeling, sensing and control are introduced and illustrated on a small two control area system. We explain the relevance of Joe Chow's work to this problem. In particular, we suggest that the early standard and non-standard form singular perturbation methods should be examined again in light of the changing technologies. The interaction variable, which is a concept motivated by non-standard form singular perturbation, is proposed to estimate the strength of the interactions among the control areas. The interaction variable-based results and conclusions are verified by the slow coherency-based approach, which had its origin in the early work of Joe Chow. Moreover, the on-line implementation of the proposed E-AGC would not be possible without the efforts made in the direction of PMUs, concentrators of the type Joe Chow recently worked on. This chapter has been written with the idea of highlighting the long-lasting impact of the methodological thinking nurtured by Joe Chow. The co-author expresses his gratitude for the life-long work which has led to this school of thinking.

Acknowledgements The authors would like to express their appreciation for the partial support for this research provided by US NSF award 0931978, PSERC S-37 and the Semiconductor Research Corporation (SRC) Smart Grid Research Center (SGRC) at Carnegie Mellon University, Research Task 2111.002.

References

1. Ilić, M.D., Zaborszky, J. Dynamics and Control of Large Electric Power Systems. Wiley-Interscience, New York (2000)
2. Chow, J.H. Time-Scale Modeling of Dynamic Networks with Applications to Power Systems. Springer-Verlag, New York (1982)
3. Kokotović, P.V., Khalil, H.K., O'Reilly, J. Singular Perturbation Methods in Control Analysis and Design. Academic Press, London (1986)
4. Winkelman, J.R., Chow, J.H., Bowler, B.C., Avramovic, B., Kokotovic, P.V. An Analysis of Interarea Dynamics of Multi-Machine Systems. Power Apparatus and Systems. IEEE Transactions on, vol.PAS-100, no.2, pp.754-763, Feb. 1981
5. Kokotović, P.V., Avramovic, B., Chow, J.H., Winkelman, J.R. Coherency based decomposition and aggregation. Automatica, vol.18, no.1, pp.47-56, 1982
6. Chow, J.H., Winkelman, J.R., Pai, M.A., Sauer, P.W. Singular perturbation analysis of large-scale power systems. International Journal of Electrical Power and Energy Systems, vol.12, no.2, pp.117-126, 1990